

**Tracking Control for a DC Microgrid Feeding Uncertain Loads in More Electric Aircraft**  
*Adaptive Backstepping Approach*

Yousefizadeh, Shirin; Bendtsen, Jan Dimon; Vafamand, Navid; Khooban, Mohammad Hassan; Blaabjerg, Frede; Dragicevic, Tomislav

*Published in:*  
I E E E Transactions on Industrial Electronics

*DOI (link to publication from Publisher):*  
[10.1109/TIE.2018.2880666](https://doi.org/10.1109/TIE.2018.2880666)

*Publication date:*  
2019

*Document Version*  
Accepted author manuscript, peer reviewed version

[Link to publication from Aalborg University](#)

*Citation for published version (APA):*  
Yousefizadeh, S., Bendtsen, J. D., Vafamand, N., Khooban, M. H., Blaabjerg, F., & Dragicevic, T. (2019). Tracking Control for a DC Microgrid Feeding Uncertain Loads in More Electric Aircraft: Adaptive Backstepping Approach. *I E E E Transactions on Industrial Electronics*, 66(7), 5644 - 5652. Article 8536921. <https://doi.org/10.1109/TIE.2018.2880666>

**General rights**

Copyright and moral rights for the publications made accessible in the public portal are retained by the authors and/or other copyright owners and it is a condition of accessing publications that users recognise and abide by the legal requirements associated with these rights.

- Users may download and print one copy of any publication from the public portal for the purpose of private study or research.
- You may not further distribute the material or use it for any profit-making activity or commercial gain
- You may freely distribute the URL identifying the publication in the public portal -

**Take down policy**

If you believe that this document breaches copyright please contact us at [vbn@aub.aau.dk](mailto:vbn@aub.aau.dk) providing details, and we will remove access to the work immediately and investigate your claim.

# Tracking Control for a DC Microgrid Feeding Uncertain Loads in More Electric Aircraft: Adaptive Backstepping Approach

Shirin Yousefizadeh, Jan Dimon Bendtsen, *Member, IEEE*, Navid Vafamand, Mohammad Hassan Khooban, *Senior Member, IEEE*, Frede Blaabjerg, *Fellow, IEEE*, and Tomislav Dragičević, *Senior Member, IEEE*

**Abstract**—More electric aircraft (MEAs) comprise a vast amount of power electronic loads, which usually behave as constant power loads (CPLs). The incremental negative impedance of CPLs threatens system stability. To ensure an effective control of power flow in MEAs, eliminating the undesired behavior of CPLs is a necessity. This aim requires spontaneous power estimation of the time-varying uncertain loads. In this paper, an adaptive backstepping controller, which is interconnected to a 3<sup>rd</sup> degree cubature Kalman filter (CKF), is developed for a DC MG feeding non-ideal CPLs. At first, the load power is considered as an artificial state and augmented into the system states, which enables estimation of not only the DC MG states but also the unknown value of the load power. The estimated load power is then forwarded to a backstepping controller. The systematic approach of this controller allows obtaining the control signal, which is the duty ratio of the switch, to not only system stabilizing but also tracking a desired voltage of the DC bus under the load power variations. The proposed adaptive controller is tested on a DC MG that has one CPL. The conducted experimental results verify the proposed nonlinear control in tracking the desired voltage of the DC bus under slow and fast variations of the load power.

**Index Terms**—More electric aircraft power system, DC microgrid (MG), Constant power load (CPL), Cubature Kalman filter (CKF), Adaptive backstepping controller.

## I. INTRODUCTION

Nowadays, driven by environmental benefits, improving systems' performance and the high price of fossil fuels, renewable energies have attracted significant research interest. Advancement of power electronic systems has also caused a trend toward the realization of more efficient electric aircrafts [1], electric ships [2], and electric vehicles [3], which are all power electronics intensive technologies. Conventional aircrafts were driven by electrical, mechanical, pneumatic, and hydraulic systems [4]. However, more electric aircraft (MEA) concept was recently introduced by the U.S. air force to encourage the electrification of aircrafts [5]. The transition

from conventional aircraft to MEA is expected to increase performance, reduces aerospace ground equipment/ground support equipment, and decreases operation and support costs [5]. Traditional aircrafts contain hydraulic, pneumatic, mechanical and electrical subsystems. The interactions between all these subsystems reduce the efficiency and reliability of the aircraft power systems [6]. Electrification of aircrafts reduces the weight, size, and fuel consumption, and increases the overall efficiency [7].

Microgrids (MG) are systems used to control the power flow of renewable energy sources, which are mainly distributed. Integration and development of MGs in the MEA is one of the challenges to be addressed [8]. Because of the advantages of DC microgrids (MG) over AC MGs, there is a tendency toward using DC MGs in MEA [9]. These advantages include power loss reduction in AC/DC power conversion [10], removing frequency control problems, improving power quality, decreasing the space and weight of transformers [9], and improving fault reconfigurability. DC MGs consist of several interconnected active loads, such as actuators and energy storage systems (ESS), which are commonly controlled by converters. If the bandwidth and control performance of these loads are considerably high, they consume power, which is independent of the bus voltage. In this case, these loads are considered as constant power loads (CPLs). CPLs then behave like incremental negative impedances, which can threaten the stability of DC MGs. Thus, minimizing the undesired effect of CPLs is a necessity to have a successful control of DC MGs.

Several strategies are proposed to mitigate the destructive effects of CPLs in DC MGs. Two basic strategies are passive damping and active damping approaches [11]. Passive damping includes adding damping resistors to the filters. Even though this approach is simple and effective, it causes a lot of dissipation. Active damping involves modifying the control loop, which acts like a virtual resistor [11]. Active damping approaches actively inject the power to the system in order to neutralize the effects of CPLs [12]. In addition, these active damping approaches, which are based on small-signal models, can ensure system stability only in the vicinity of the operating point. Therefore, these linear control methods are not useful in the case of occurrence of large variations in the system [12]. Several nonlinear control approaches have also been studied the stability problems with the DC MGs containing CPLs. In [13], a model predictive control (MPC) is employed, by minimizing a user-defined performance index, to control

S. Yousefizadeh and J.D. Bendtsen are with the Department of Electronic Systems, Aalborg University, Aalborg, Denmark.

N. Vafamand, M.H. Khooban, F. Blaabjerg, and T. Dragičević are with the Energy Technology Department, Aalborg University, Aalborg, Denmark. Corresponding author email: shy@es.aau.dk

switching of a boost converter sourcing a CPL. However, MPC is not suitable for plant-wide real-time applications, due to its computational burden [14]. In [15], a sliding mode controller is proposed to stabilize a boost converter sourcing a CPL by controlling the duty ratio. This method is able to stabilize the system over the whole operating range even when the load power and supply voltage vary significantly. However, this method requires measuring the capacitor current, which is costly and causes ripple filtering degradation and the output impedance increasing [12]. Backstepping control is a systematic approach to design adaptive controllers with a simple implementation. This method guarantees global or local stabilization and accurate tracking in the presence of uncertainties. In addition, it permits retaining useful nonlinearities, which improves the controller performance [16]. Recently, employing the backstepping controller in the presence of CPLs is considered in [12]. In cases where unknown or time-varying parameters are present in the system, adaptive control approaches, which can regulate the adaptive parameters on-line, have attracted attention [17], [18]. In [19], an adaptive backstepping control is proposed to solve the tracking problem in an electric vehicle. In [12], a deterministic nonlinear disturbance observer is employed to estimate the uncertain power of the load, which is then used in an adaptive backstepping controller to track the DC bus voltage. Nonetheless, the deterministic observer performance may deteriorate in the presence of noisy measurements, which makes it unsuitable for practical applications [20]. Furthermore, the approach of [12] is sensitive to system uncertainty and unmodeled dynamics. Kalman filtering approaches are proved to be optimal in the case of linear dynamics and Gaussian noise [21]. The extended Kalman filter (EKF) applies the Kalman filter to nonlinear systems by linearizing the system model. The EKF exhibits poor performance for highly nonlinear dynamic systems. However, Bayesian sampling methods are alternatives to the EKF. These methods are divided into random sampling and deterministic sampling [22]. Random sampling methods involve a high computational burden, which makes them inappropriate for practical applications where fast estimation is required. Among the deterministic sampling methods, cubature Kalman filters (CKFs) have attracted particular interest recently due to their attractive features such as accuracy, lower computational burden, and good numerical stability properties [22]–[24].

In this paper, to eliminate the undesired effects of CPLs in the MEA operation, a 3<sup>rd</sup> degree CKF algorithm is developed to solve a joint estimation problem to estimate not only DC MG's states but also the total power of the load. To achieve this goal, the CPL's power is augmented into the state space vector of the system as a virtual state. The estimated load power is then forwarded to a backstepping controller to both stabilize the system and also to track a desired voltage on the DC bus. To this aim, first the strict-feedback model of the system model is constructed. By following the recursive backstepping controller steps to obtain the intermediate control laws, the main control law, which governs the duty ratio of the switch, is obtained. In comparison to the work in [12], this approach is robust against system uncertainties, unmodeled dynamics, and noisy measurements. Moreover, the backstepping controller is designed based on more simple

control Lyapunov functions (CLF), which makes the controller design procedure simpler and easier to be used on the more complex system models. The developed adaptive backstepping controller is then applied to a DC MG connected to an uncertain time-varying CPL. The effectiveness of our proposed CKF to estimate the unknown time-varying power of the total load and the proposed backstepping controller to stabilize the system and track the voltage of the DC bus is verified by experiments.

The outline of this paper is as follows. The modeling of the DC MG is provided in Section II. In Section III, the developed CKF algorithm for the estimation of the unknown power of the load is presented. Section IV presents the nonlinear backstepping controller design, which is interconnected to the estimated power of the load in Section III. To investigate the performance of the proposed adaptive backstepping controller, the illustrative experimental results are presented in sections V. Finally, Section VI concludes the paper.

## II. MEA DC MICROGRID DYNAMIC

A typical MEA is shown in Fig. 1 and its simplified electrical schematic is shown in Fig. 2.

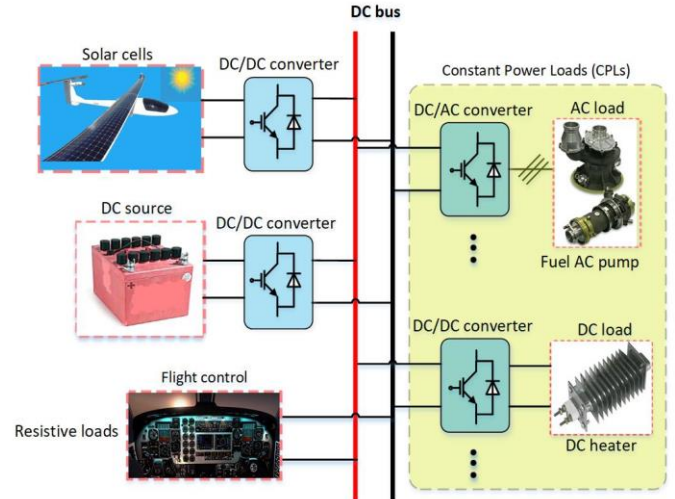


Fig. 1. Power system illustration of an MEA DC MG.

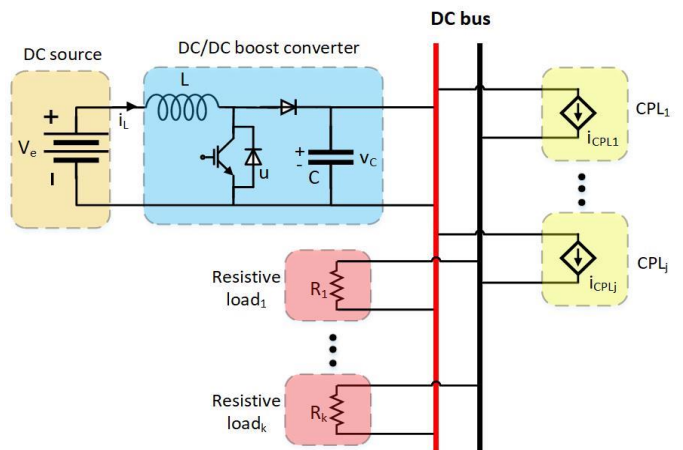


Fig. 2. A simplified illustration of the MEA DC MG shown in Fig. 1 with  $Q$  CPLs and  $K$  resistive loads.

It has several CPLs, solar cells for providing power during

the day and batteries for providing power during the night. In MEA, most of the closed-loop DC and AC loads behave as CPLs [25]. An example of AC CPLs is a DC/AC converter drives a fuel AC pump when the fuel pump tightly supplies a constant flow of fuel to the engines. Another example of an AC CPL is a DC/AC converter connected to an electric motor that tightly regulates the motor speed [26], [27]. An example of a DC CPL is a heater, for which it is required to keep the dissipated power from the heater constant, in spite of changes in the resistor temperature and process variations. These heaters can have different applications, such as maintaining warmth at high altitudes and in cold weather and food warming.

As can be seen in Fig. 2, all the resistive loads,  $R_1, \dots, R_K$ , are in parallel and the equivalent resistive load,  $R$ , is defined as

$$R = \left( \frac{1}{R_1} + \dots + \frac{1}{R_K} \right)^{-1} \quad (1)$$

The circuit diagram of Fig. 2 is shown in Fig. 3. In this diagram, the CPL current is described as

$$i_{CPL} = \frac{P_{CPL}}{v_{CPL}} = \frac{P_{CPL}}{v_C} \quad (2)$$

where  $v_{CPL}$ ,  $P_{CPL}$  are the CPL voltage and power, respectively, and  $v_C$  is the capacitor voltage.

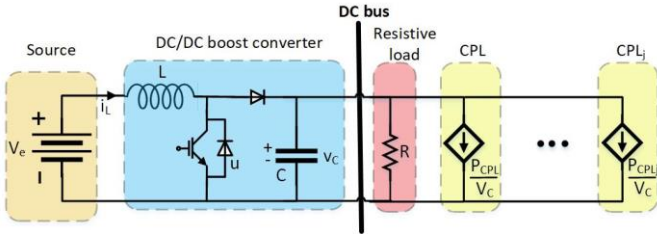


Fig. 3. Circuit Diagram of the DC MG shown in Fig. 2 with Q CPLs and K resistive loads.

The DC/DC boost converter in Fig. 3 can be represented by a switch, as depicted in Fig. 4.

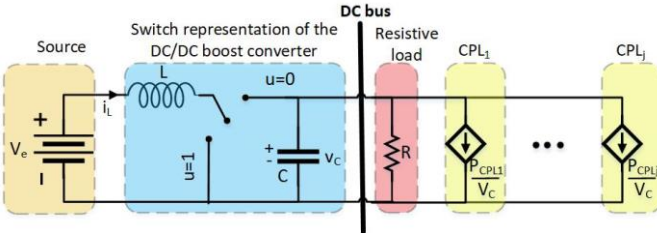


Fig. 4. Switch representation of the simplified power converter load as a CPL.

In Fig. 4,  $u \in \{0,1\}$  is the duty cycle of the switch and the control signal of the system.  $u = 0$  corresponds to the conducting mode for the switch and  $u = 1$  corresponds to the non-conducting mode for the switch. The total load includes the resistive loads and the CPLs. The dynamical model of the system in Fig. 4 is obtained through employing the Kirchhoff's current and voltage laws as follows:

$$\begin{cases} L \frac{di_L}{dt} = V_e - (1-u)v_C \\ C \frac{dv_C}{dt} = (1-u)i_L - \frac{v_C}{R} - \frac{P_{CPL1}}{v_C} - \dots - \frac{P_{CPLQ}}{v_C} \end{cases} \quad (3)$$

where  $L, C$  are the input inductance and capacitance, respectively,  $i_L$  is the inductance current,  $V_e$  is the source

voltage, and  $P_{CPL1}, \dots, P_{CPLQ}$  are the power of the CPLs. In the above equations,  $i_L, v_C$  are measurable. Also, the total power of the load,  $P_{load}$ , as defined below, is estimated using the CKF approach as explained thereafter.

$$P_{load} = P_{CPL1} + \dots + P_{CPLQ} + \frac{v_C^2}{R} \quad (4)$$

Then, the control signal,  $u$ , is obtained by applying the backstepping control as explained in section IV.

### III. CUBATURE KALMAN FILTER FOR POWER ESTIMATION

This section presents the design procedure of the developed 3<sup>rd</sup> degree CKF to estimate the unknown power of the total load [28]. To this aim, the unknown vector of the total load's power,  $P_{load}$ , is augmented in the states of the system, in (3) [4]. Thereby, the augmented state vector is defined as:

$$x = [i_L \ v_C \ P_{load}]^T \quad (5)$$

Since the  $P_{load}$  dynamic is unknown, it is assumed that  $\dot{P}_{load} = 0$ . Using (3), the augmented state-space model for the DC MG is

$$\dot{x} = [i_L \ v_C \ P_{load}]^T = f(x, u) \quad (6)$$

Also, the system measurements are described as

$$y = \begin{bmatrix} I \\ 0 \end{bmatrix} [i_L \ v_C \ P_{load}]^T = Hx \quad (7)$$

Putting (6), (7) together and considering system and measurement noises,  $w$  and  $v$ , respectively, yields to

$$\begin{cases} \dot{x} = f(x, u) + w \\ y = Hx + v \end{cases} \quad (8)$$

where  $w$  and  $v$  are assumed independent and normally distributed with zero mean and known covariance matrices  $Q$  and  $R$ , respectively. The obtained state-space model can be discretized using the forward Euler method as

$$\begin{cases} x_{k+1} = x_k + T_s f(x_k, u_k) + w_k \\ y_k = Hx_k + v_k \end{cases} \quad (9)$$

where  $T_s$  is the discretizing time and  $k$  is a discrete sample number. The 3<sup>rd</sup> degree CKF algorithm is done by recursively performing time update and measurement update. After convergence of the filter, the last element of the estimated state is the estimated power of the CPL. The CKF steps are as follows [29]:

#### • Time update

1. Factorize  $\mathcal{P}_{k-1|k-1}$  by Cholesky decomposition

$$\mathcal{P}_{k-1|k-1} = S_{k-1|k-1} S_{k-1|k-1}^T \quad (10)$$

2. Calculate cubature points for  $i = 1, \dots, 2n$

$$X_{i,k-1|k-1} = S_{k-1|k-1} \zeta_i + \hat{x}_{k-1|k-1} \quad (11)$$

3. Propagate cubature points by the nonlinear model

$$X_{i,k|k-1}^* = F(X_{i,k-1|k-1}, u_{k-1}) \quad (12)$$

4. Estimate the predicted states

$$\hat{x}_{k|k-1} = \frac{1}{2n} \sum_{i=1}^{2n} X_{i,k|k-1}^* \quad (13)$$

5. Estimate the predicted covariance of the states

$$\begin{aligned} \mathcal{P}_{k|k-1} &= \frac{1}{2n} \sum_{i=1}^{2n} (X_{i,k|k-1}^* - \hat{x}_{k|k-1})(X_{i,k|k-1}^* - \hat{x}_{k|k-1})^T \\ &\quad + Q_{k-1} \end{aligned} \quad (14)$$

#### • Measurement update

1. Factorize  $\mathcal{P}_{k|k-1}$  by Cholesky decomposition

$$\mathcal{P}_{k|k-1} = S_{k|k-1} S_{k|k-1}^T \quad (15)$$

2. Calculate cubature points for  $i = 1, \dots, 2n$

$$X_{i,k-1|k-1} = S_{k|k-1} \zeta_i + \hat{x}_{k|k-1} \quad \text{for } i = 1, \dots, 2n \quad (16)$$

3. Propagate cubature points by the measurement model

$$Y_{i,k|k-1} = h(X_{i,k|k-1}, u_k) \quad (17)$$

4. Estimate the predicted measurements

$$\hat{y}_{k|k-1} = \frac{1}{2n} \sum_{i=1}^{2n} Y_{i,k|k-1} \quad (18)$$

5. Estimate the auto-covariance matrix:

$$\begin{aligned} \mathcal{P}_{yy,k|k-1} &= \frac{1}{2n} \sum_{i=1}^{2n} (Y_{i,k|k-1} - \hat{y}_{k|k-1}) \\ &\quad \times (Y_{i,k|k-1} - \hat{y}_{k|k-1})^T + R_k \end{aligned} \quad (19)$$

6. Estimate the cross-covariance matrix

$$\begin{aligned} \mathcal{P}_{xy,k|k-1} &= \frac{1}{2n} \sum_{i=1}^{2n} (X_{i,k|k-1} - \hat{x}_{k|k-1}) \\ &\quad \times (Y_{i,k|k-1} - \hat{y}_{k|k-1})^T + R_k \end{aligned} \quad (20)$$

7. Estimate the Kalman gain

$$K_k = \mathcal{P}_{xy,k|k} \mathcal{P}_{yy,k|k}^{-1} \quad (21)$$

8. Estimate the updated states

$$\hat{x}_{k|k} = \hat{x}_{k|k-1} + K_k (y_k - \hat{y}_{k|k-1}) \quad (22)$$

9. Estimate the covariance of the states

$$\mathcal{P}_{k|k} = \mathcal{P}_{k|k-1} + K_k \mathcal{P}_{yy,k|k} K_k^T \quad (23)$$

Using the CKF and having  $i_L, v_C$  measurements, the estimate of  $P_{load}$  is then simply extracted from the estimated state vector  $\hat{x}$ .

#### IV. ADAPTIVE BACKSTEPPING CONTROLLER

In this section, the procedure of designing the backstepping controller is presented. The control objective is to find the value of the switch position function that stabilizes the output voltage of the converter,  $v_C$ , toward its desired value,  $v_{Cd}$ . The control signal is then used to generate PWM gate signals for the converter [15]. To implement the backstepping controller, first, the state space of the system in (3) is transformed to the standard strict-feedback form for designing the backstepping controller. The steps for the proposed backstepping controller are provided below:

##### Step 1: Strict-feedback form of the system

To obtain the strict-feedback form of the system, based on the results of [12], the following diffeomorphism is applied to the dynamical model of the system in (3):

$$z_1 = \frac{1}{2} L i_L^2 + \frac{1}{2} C v_C^2 \quad (24)$$

where  $z_1$  is the total stored energy in the system. By knowing the fact that the control objective is asymptotic convergence of  $v_C$ , toward its desired value,  $v_{Cd}$ , the desired values for the inductor current,  $i_{Ld}$ , can be obtained as:

$$i_{Ld} = \frac{P_d}{V_e} \quad (25)$$

where  $P_d$  is the power of the total load that expressed as

$$P_d = P_{CPL} + \frac{v_{Cd}^2}{R} \quad (26)$$

Therefore, the desired value of  $z_1$  can be expressed as

$$z_{1d} = \frac{1}{2} L i_{Ld}^2 + \frac{1}{2} C v_{Cd}^2 \quad (27)$$

The tracking error is defined as

$$e_1 = z_1 - z_{1d} \quad (28)$$

which can be simplified as

$$e_1 = \frac{1}{2} L (i_L^2 - i_{Ld}^2) + \frac{1}{2} C (v_C^2 - v_{Cd}^2) \quad (29)$$

The derivative of the tracking error is as

$$\dot{e}_1 = L i_L \frac{di_L}{dt} + C v_C \frac{dv_C}{dt} \quad (30)$$

which, by using (3), can be simplified as

$$\dot{e}_1 = V_e i_L - \frac{v_C^2}{R} - P_{CPL} \quad (31)$$

Since the total power of the load is estimated using the CKF, (31) is rewritten as

$$\dot{e}_1 = V_e i_L - \frac{v_C^2}{R} - P_{CPL} + \frac{v_C^2}{R_0} - \frac{v_C^2}{R_0} \quad (32)$$

where  $R_0$  is the nominal resistance of the resistive load. Based on (32), the new state  $z_2$  is defined as  $z_2 = V_e i_L - \frac{v_C^2}{R_0}$  and the uncertain term  $d_1 = -\frac{v_C^2}{R} - P_{CPL} + \frac{v_C^2}{R_0}$ . Taking the derivative of  $z_2$  results in

$$\dot{z}_2 = V_e \frac{di_L}{dt} - \frac{2}{R_0} v_C \frac{dv_C}{dt} \quad (33)$$

which can be rewritten as

$$\dot{z}_2 = \frac{V_e^2}{L} - (1-u) \left( \frac{V_e v_C}{L} + \frac{2v_C i_L}{R_0 C} \right) + \frac{2}{R_0 C} (P_{CPL} + \frac{v_C^2}{R}) \quad (34)$$

In order to separate the uncertain term of the total power of the load, (34) is rewritten as

$$\begin{aligned} \dot{z}_2 &= \frac{V_e^2}{L} - (1-u) \left( \frac{V_e v_C}{L} + \frac{2v_C i_L}{R_0 C} \right) + \frac{2}{R_0 C} (P_{CPL} \\ &\quad + \frac{v_C^2}{R} + \frac{v_C^2}{R_0} - \frac{v_C^2}{R_0}) \end{aligned} \quad (35)$$

Then, based on (35),  $d_2$  and  $v$  are defined as

$$d_2 = \frac{2}{R_0 C} (P_{CPL} + \frac{v_C^2}{R} - \frac{v_C^2}{R_0}) \quad (36)$$

$$v = \frac{V_e^2}{L} - (1-u) \left( \frac{V_e v_C}{L} + \frac{2v_C i_L}{R_0 C} \right) + \frac{2v_C^2}{R_0^2 C}$$

Hence, the system model in (3) is transformed to the strict-feedback form as

$$\begin{cases} \dot{e}_1 = z_2 + d_1 \\ \dot{z}_2 = v + d_2 \end{cases} \quad (37)$$

The intermediate control law,  $v$ , can be obtained by solving the equation (37). Then the final control law,  $u$ , can be obtained from (36) as

$$u = 1 - \left( \frac{V_e^2}{L} + \frac{2v_C^2}{R^2 C} - v \right) / \left( \frac{V_e v_C}{L} + \frac{2v_C i_L}{R C} \right) \quad (38)$$

##### Step 2: Backstepping Procedure

Considering (37), the control law,  $u$ , can be obtained by employing the following procedure:

###### i. Finding the virtual control expression $z_{2d}$

Considering the first equation of (37), i.e.  $\dot{e}_1 = z_2 + d_1$ , the designed control Lyapunov function (CLF) is as  $V_1 = \frac{1}{2} e_1^2$ .



The derivative of the considered CLF is as

$$\dot{V}_1 = e_1 \dot{e}_1 = e_1(z_2 + d_1) \quad (39)$$

For asymptotic convergence of  $e_1$  toward the origin, it is required that  $\dot{V}_1 < 0$  when  $z_1 \neq 0$ . Considering  $z_{2d} = -d_1 - \zeta e_1$  where  $k$  is a positive gain matrix, results in  $\dot{V}_1 = -\zeta e_1^2 < 0$ . The new state variable  $e_2$  is defined as

$$e_2 = z_2 - z_{2d} = z_2 + d_1 + \zeta e_1 \quad (40)$$

which gives

$$z_2 = e_2 - d_1 - \zeta e_1 \quad (41)$$

Substituting (41) in  $\dot{e}_1 = z_2 + d_1$  yields

$$\begin{cases} \dot{e}_1 = e_2 - \zeta e_1 \\ \dot{e}_2 = \dot{z}_2 + \dot{d}_1 + \zeta \dot{e}_1 = v + d_2 + \dot{d}_1 + k(e_2 - \zeta e_1) \end{cases} \quad (42)$$

Defining

$$v' = v + d_2 + \dot{d}_1 \quad (43)$$

results in

$$\begin{cases} \dot{e}_1 = e_2 - \zeta e_1 \\ \dot{e}_2 = v' + \zeta e_2 - \zeta^2 e_1 \end{cases} \quad (44)$$

The next step is finding the control expression  $v'$ ; then, the intermediate control law,  $v$ , can be obtained from (43) as

$$v = v' - d_2 - \dot{d}_1 \quad (45)$$

## ii. Finding the control expression $v'$

Based on (44), the considered CLF is as  $V_2 = \frac{1}{2} e_1^2 + \frac{1}{2} e_2^2$ .

The derivative of  $V_2$  along its trajectory can be obtained as

$$\dot{V}_2 = e_1 \dot{e}_1 + e_2 \dot{e}_2 = -\zeta e_1^2 + e_2(v' + \zeta e_2 - \zeta^2 e_1 + e_1) \quad (46)$$

For asymptotic convergence of  $e_2$  toward the origin, it is needed that  $\dot{V}_2 < 0$  when  $e_2 \neq 0$ . Considering

$$v' = -(m + \zeta)e_2 + (\zeta^2 - 1)e_1 \quad (47)$$

where  $m$  is a positive gain matrix, yields to

$$\dot{V}_2 = -\zeta e_1^2 - m e_2^2 < 0 \quad (48)$$

Using (29) and (40), (47) can be simplified as

$$v' = -(m + \zeta)(z_2 + d_1) - (1 + m\zeta) \left( \frac{1}{2} L(i_L^2 - i_{Ld}^2) + \frac{1}{2} C(v_C^2 - v_{Cd}^2) \right) \quad (49)$$

The final step is finding  $v$ , and consequently,  $u$  from the obtained expression for  $v'$ .

## iii. Finding the control input $u$

Considering (45) and (49), the intermediate control law,  $v$ , can be obtained as

$$v = -(m + \zeta)(z_2 + d_1) + (-1 - m\zeta) \left( \frac{1}{2} L(i_L^2 - i_{Ld}^2) + \frac{1}{2} C(v_C^2 - v_{Cd}^2) \right) - d_2 - \dot{d}_1 \quad (50)$$

In the above equation,  $v_C$  and  $i_{Ld}$  are measurable and their instantaneous values are estimated using the CKF. Also, the only unknown quantity in  $d_1$  and  $d_2$  is  $P_{load}$ , which is estimated during operation using the CKF, and the derivative of  $d_1$  is a known value too. Therefore, all parameters in (50) are known and  $u$  can be obtained based on (38).

Also, (48) indicates the negative definiteness of the time derivative of the Lyapunov function  $V_2$ . Therefore, the errors  $e_1$  and  $e_2$  asymptotically converge to zero. Consequently, from the diffeomorphism variable changes  $z_1$  and  $z_2$ , one can infer that if the artificial states  $z_1$  and  $z_2$  converge to their desired values, then the actual system states  $i_L$  and  $v_C$  will also

converge to their desired references. Thereby, the tracking of the overall closed-loop system is assured.

## V. EXPERIMENTAL RESULTS

In this section, the results of the proposed adaptive backstepping controller are provided. The controller is integrated to the CKF algorithm, which estimates the uncertain time-varying total power of the load. The general configuration of the experimental setup is shown in Fig. 5.



Fig. 5. The experimental setup

At first, the total power of the load,  $P_{load}$ , is estimated using the CKF. Then, the estimated  $P_{load}$  serves as an input to the backstepping controller. A block diagram of the suggested approach is shown in Fig. 6.

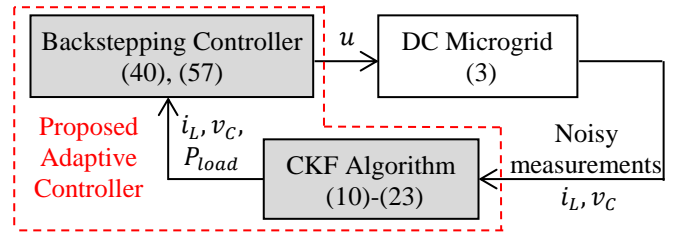


Fig. 6. A simple block diagram illustration of the proposed controller.

As can be seen in Fig. 6, the CKF algorithm is utilized to estimate  $P_{load}$  online. Then, this estimation alongside the measurements, i.e.  $i_L, v_C$ , is used in the backstepping controller to compute the optimal value of the duty cycle of the switch, i.e.  $u$ . The MG parameters are listed in Table I. The initial condition of the CKF  $\hat{x}_0 = [1 \ 55 \ 80]^T$ .

TABLE I PARAMETERS FOR THE DC MG WITH ONE CPL	
$L = 1 \text{ mH}$	$v_{Cd} = 270 \text{ V}$
$C = 470 \text{ }\mu\text{F}$	$V_e = 200 \text{ V}$

**Remark 1:** The process noise covariance matrix, i.e.  $Q$ , corresponds to both system noise covariance and the uncertainty that is expected in the state-space equations. If one is very confident in the model,  $Q$  can be small. However, there is typically some uncertainty in the model equations, such as discretization, approximations in the derivation, etc. Additionally, larger (smaller) values of  $Q$  correspond to faster (slower) convergence at the expense of larger (smaller) steady-state error [30]. Since the last element correspond to  $P_{load}$ , for which the dynamics is unknown, a larger value of system noise covariance is required. Therefore,  $R = \text{diag}(10^{-2}, 10^{-2})$  and  $Q = \text{diag}(10^{-3}, 10^{-3}, 0.3)$ . Usually, the initial value of  $p$  is chosen as a diagonal matrix whose diagonal elements are related to the expected variance of the corresponding state. Since  $i_L, v_C$  are measurable, one can choose small corresponding covariance values. On the other hand,  $P_{load}$  is unknown. Consequently, its corresponding

elements of  $p$  should have a larger value. Therefore, the initial value of  $p$  is chosen as  $p_0 = \text{diag}(1, 1, 10^3)$ .

**Remark 2:** Since the estimation of  $P_{load}$  through the CKF algorithm is fed to the controller, the CKF should be faster than the controller. As can be seen in (38) and (50), since the sum of the backstepping controller parameters, i.e.  $m, \zeta$ , appears in the control signal, the control parameters have the same effect on the control signal. Larger parameters lead to a smaller settling time. However, since  $m + \zeta$  is multiplied to the measurement signals, larger values of  $m + \zeta$  tend to amplify the noise in these signals. Nonetheless, some part of the amplified noise can be compensated for by the measurement covariance matrix,  $R$ , in the CKF. In addition, very high values of  $m + \zeta$  cause system overshoot. Overall, in tuning the controller alongside the CKF parameters, there is a trade-off between a faster response, less overshoot, and more robustness to noise. Considering all these facts,  $m, \zeta$  are chosen in the subsequent experiments as  $m + \zeta = 400$ .

To show the merits of the proposed nonlinear controller, two scenarios are provided. In the first one, the power of the total load,  $P_{load}$ , changes in a stepwise manner; meanwhile, in the second scenario, the power of the total load varies slightly and periodically. In the following, the experimental results for both scenarios are presented. In both scenarios, the CKF algorithm is used to estimate the unknown load power and then the adaptive backstepping controller regulated the voltage of the DC MG to the desired reference of 270 (V). The scale of each figure is given together with it and the horizontal axis shows the time in the interval  $t \in [0, 6]$  seconds.

**Scenario 1 (Stepwise varying  $P_{load}$ ):** In this scenario,  $P_{load}$  changes promptly at some moments. These sudden changes can be reasonable in practice, when the characteristics of the loads connected to inverters changes very fast. By applying the CKF, the currents and voltages of the filter, as well as the total load's power are estimated. Fig. 7 shows the actual values and the estimations of the augmented states using the CKF. As can be seen in Fig. 7, the suggested observer can estimate the  $P_{load}$  value fast and precisely. From Fig. 7, one concludes that by promptly changing the power of the CPL, a sudden error is produced in the CKF estimation, which however is attenuated very fast. After that, since the power is constant, the estimation error of the states becomes smaller. Then, the estimated states using the CKF are employed in the backstepping controller.

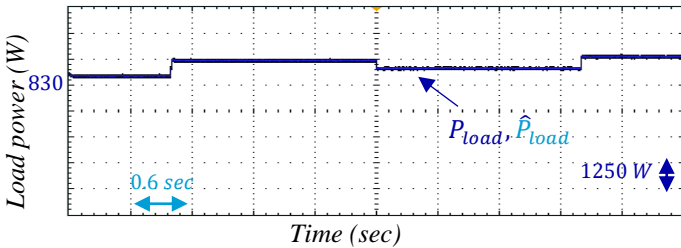


Fig. 7. The actual value and the estimation of the load's power using the CKF of Scenario 1.

As can be seen in Fig. 8, the proposed controller (38) tracks the desired value of the output voltage of the converter.

**Scenario 2 (periodic slowly varying  $P_{load}$ ):** In this

scenario, the total power of the load changes slowly and periodically. In practice, the slowly variation of  $P_{load}$  is occurred because the efficiency of practical converters is not constant and the controller of the converters has a limited bandwidth. Fig. 9 shows the actual values and estimations of the augmented states of the CKF.

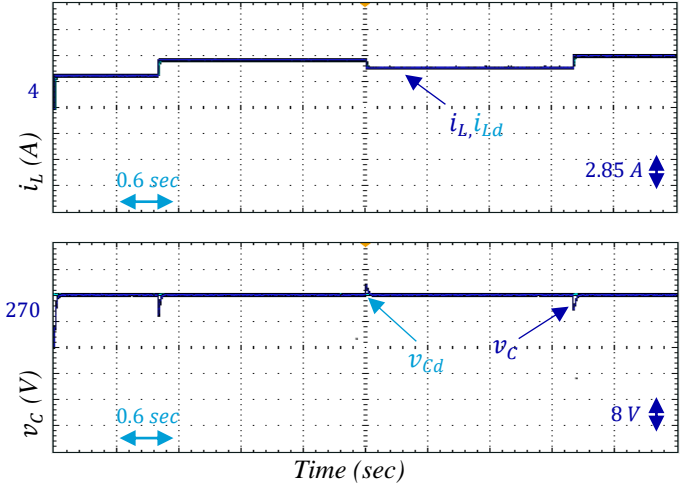


Fig. 8. The desired values of  $v_c$  and  $i_L$  and their obtained value using the backstepping controller of Scenario 1.

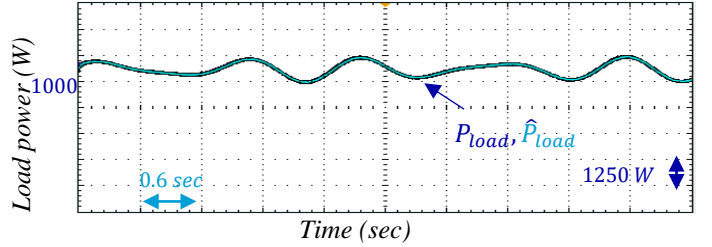


Fig. 9. The actual value and the estimation of the load's power using the CKF of Scenario 2.

As can be seen in Fig. 9, the suggested observer estimates the value of  $P_{load}$  effectively. The CKF captures the varying behavior of the DC MG with continuously varying power load and results in a small estimation error. Then, the estimated states using the CKF are employed in the backstepping controller. As can be seen in Fig. 10, the proposed controller tracks the desired value of the output voltage of the converter.

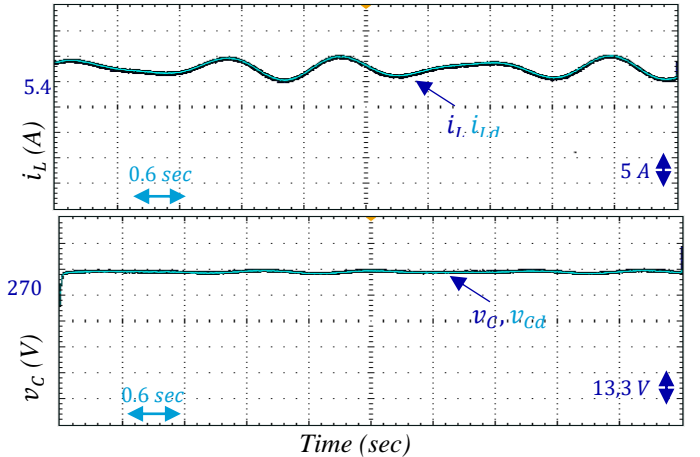


Fig. 10. The desired values of  $v_c$  and  $i_L$  and their obtained value using the backstepping controller of Scenario 2.

## VI. CONCLUSION

The goal of this research was to stabilize a DC MG that has uncertain time-varying loads and to make the DC voltage of the bus to track the desired voltage. To this aim, the uncertain load power was augmented to the system states vector and its spontaneous value is estimated using a cubature Kalman filter (CKF). The estimated load power is then feedforwarded to a backstepping controller to obtain the duty ratio of the switch. To implement the controller, first, the strict-feedback model of the system is obtained. Then, the virtual control signals are obtained step by step, by constructing suitable control Lyapunov functions (CLF) and providing the stability conditions, until the desired control signal is obtained. To illustrate the effectiveness of the proposed controller, two scenarios including fast changes and slow periodically changes of the load power are provided. The real-time implementation results showed the ability of the proposed adaptive controller in tracking the desired voltage of the bus for sudden and continuous changes of the load power.

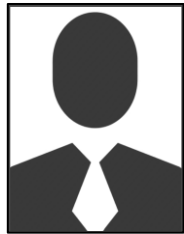
## REFERENCES

- [1] A. Eid, H. El-Kishky, M. Abdel-Salam, and M. T. El-Mohandes, "On power quality of variable-speed constant-frequency aircraft electric power systems," *IEEE Transactions on Power Delivery*, vol. 25, DOI: 10.1109/TPWRD.2009.2031672, no. 1, pp. 55–65, 2010.
- [2] "Shipboard Microgrids: A Novel Approach to Load Frequency Control," *IEEE Transactions on Sustainable Energy*, vol. 9, DOI: 10.1109/TSTE.2017.2763605, no. 2, pp. 843–852, Apr. 2018.
- [3] M. H. Khooban, N. Vafamand, T. Niknam, T. Dragicevic, and F. Blaabjerg, "Model-predictive control based on Takagi-Sugeno fuzzy model for electrical vehicles delayed model," *IET Electric Power Applications*, vol. 11, DOI: 10.1049/iet-epa.2016.0508, no. 5, pp. 918–934, 2017.
- [4] K. Emadi and M. Ehsani, "Aircraft power systems: technology, state of the art, and future trends," *IEEE Aerospace and Electronic Systems Magazine*, vol. 15, DOI: 10.1109/62.821660, no. 1, pp. 28–32, Jan. 2000.
- [5] R. E. J. Quigley, "More Electric Aircraft," in *Proceedings of Eighth Annual Applied Power Electronics Conference and Exposition*, DOI: 10.1109/APEC.1993.290667, pp. 906–911, March 1993.
- [6] S. Yin, K. J. Tseng, R. Simanjorang, Y. Liu, and J. Pou, "A 50-kW High-Frequency and High-Efficiency SiC Voltage Source Inverter for More Electric Aircraft," *IEEE Transactions on Industrial Electronics*, vol. 64, DOI: 10.1109/TIE.2017.2696490, no. 11, pp. 9124–9134, Nov. 2017.
- [7] J. Benzaquen, M. B. Shadmand, A. Stonestreet, and B. Mirafzal, "A unity power factor active rectifier with optimum space-vector predictive DC voltage control for variable frequency supply suitable for more electric aircraft applications," in *2018 IEEE Applied Power Electronics Conference and Exposition (APEC)*, San Antonio, TX, USA, 2018, pp. 1455–1460.
- [8] P. Magne, B. Nahid-Mobarakeh, and S. Pierfederici, "Dynamic Consideration of DC Microgrids With Constant Power Loads and Active Damping System; A Design Method for Fault-Tolerant Stabilizing System," *IEEE Journal of Emerging and Selected Topics in Power Electronics*, vol. 2, DOI: 10.1109/JESTPE.2014.2305979, no. 3, pp. 562–570, Sep. 2014.
- [9] Z. Jin, G. Sulligoi, R. Cuzner, L. Meng, J. C. Vasquez, and J. M. Guerrero, "Next-Generation Shipboard DC Power System: Introduction Smart Grid and dc Microgrid Technologies into Maritime Electrical Networks," *IEEE Electrification Magazine*, vol. 4, DOI: 10.1109/MELE.2016.2544203, no. 2, pp. 45–57, Jun. 2016.
- [10] T. Dragičević, X. Lu, J. C. Vasquez, and J. M. Guerrero, "DC Microgrids-Part II: A Review of Power Architectures, Applications, and Standardization Issues," *IEEE Transactions on Power Electronics*, vol. 31, DOI: 10.1109/TPEL.2015.2464277, no. 5, pp. 3528–3549, May 2016.
- [11] L. Ding, Q. L. Han, L. Y. Wang, and E. Sindi, "Distributed Cooperative Optimal Control of DC Microgrids with Communication Delays," *IEEE Transactions on Industrial Informatics*, vol. 14, DOI: 10.1109/TII.2018.2799239, no. 9, pp. 3924–3935, Sept. 2018.
- [12] A. M. Rahimi and A. Emadi, "Active Damping in DC/DC Power Electronic Converters: A Novel Method to Overcome the Problems of Constant Power Loads," *IEEE Transactions on Industrial Electronics*, vol. 56, DOI: 10.1109/TIE.2009.2013748, no. 5, pp. 1428–1439, May 2009.
- [13] T. Dragicevic, "Dynamic Stabilization of DC Microgrids with Predictive Control of Point of Load Converters," *IEEE Transactions on Power Electronics*, vol. 33, DOI: 10.1109/TPEL.2018.2801886, no. 12, pp. 10872–10884, 2018.
- [14] R. Cheng, J. F. Forbes, and W. S. Yip, "Price-driven coordination method for solving plant-wide MPC problems," *Journal of Process Control*, vol. 17, DOI: 10.1016/j.jprocont.2006.04.003, no. 5, pp. 429–438, Jun. 2007.
- [15] Y. Zhao, W. Qiao, and D. Ha, "A Sliding-Mode Duty-Ratio Controller for DC/DC Buck Converters With Constant Power Loads," *IEEE Transactions on Industry Applications*, vol. 50, no. 2, pp. 1448–1458, Mar. 2014.
- [16] J. Zhou and C. Wen, *Adaptive Backstepping Control of Uncertain Systems: Nonsmooth Nonlinearities, Interactions or Time-Variations*. Berlin Heidelberg: Springer-Verlag, Springer, 2008, DOI: 10.1007/978-3-540-77807-3.
- [17] H. Li, L. Wang, H. Du, and A. Boukroune, "Adaptive fuzzy backstepping tracking control for strict-feedback systems with input delay," *IEEE Trans. Fuzzy Syst.*, vol. 25, DOI: 10.1109/TFUZZ.2016.2567457, no. 3, pp. 642–652, June 2017.
- [18] Y.-J. Liu and T. Shaocheng, "Barrier Lyapunov functions for Nussbaum gain adaptive control of full state constrained nonlinear systems," DOI: <https://doi.org/10.1016/j.automatica.2016.10.011>, vol. 76, pp. 143–152, 2017.
- [19] J. Yu, Y. Ma, Y. Haisheng, and L. Chong, "Adaptive fuzzy dynamic surface control for induction motors with iron losses in electric vehicle drive systems via backstepping," DOI: <https://doi.org/10.1016/j.ins.2016.10.018>, vol. 376, pp. 172–189, 2017.
- [20] C. Mitsantisuk, K. Ohishi, S. Urushihara, and S. Katsura, "Kalman filter-based disturbance observer and its applications to sensorless force control," *Advanced Robotics*, vol. 25, DOI: <https://doi.org/10.1163/016918610X552141>, no. 3–4, pp. 335–353, 2011.
- [21] D. Simon, *Optimal state estimation: Kalman, H<sub>∞</sub> and nonlinear approaches*. Hoboken, N.J: Wiley-Interscience, 2006.
- [22] Z. Xin-Chun and G. Cheng-Jun, "Cubature Kalman filters: Derivation and extension," *Chinese Phys. B*, vol. 22, DOI: 10.1088/1674-1056/22/12/128401, no. 12, p. 128401, 2013.
- [23] E. Shokri and J. Zarei, "Convergence analysis of non-linear filtering based on cubature Kalman filter," *IET Science, Measurement & Technology*, vol. 9, DOI: 10.1049/iet-smt.2014.0056, no. 3, pp. 294–305, May 2015.
- [24] M. A. Kardan *et al.*, "Improved Stabilization of Nonlinear DC Microgrids: Cubature Kalman Filter Approach," *IEEE Transactions on Industry Applications*, vol. 54, DOI: 10.1109/TIA.2018.2848959, no. 5, pp. 5104–5112, Oct. 2018.
- [25] X. Liu, Y. Zhou, and S. Ma, "EMI filter design for constant power loads in more electric aircraft power systems," in *2009 IEEE 6th International Power Electronics and Motion Control Conference*, DOI: 10.1109/IPEMC.2009.5157858, pp. 2664–2668, July 2009.
- [26] A. Emadi, A. Khaligh, C. H. Rivetta, and G. A. Williamson, "Constant power loads and negative impedance instability in automotive systems: definition, modeling, stability, and control of power electronic converters and motor drives," *IEEE Transactions on Vehicular Technology*, vol. 55, DOI: 10.1109/TVT.2006.877483, no. 4, pp. 1112–1125, Jul. 2006.
- [27] N. Vafamand, M. H. Khooban, T. Dragicevic, and F. Blaabjerg, "Networked Fuzzy Predictive Control of Power Buffers for Dynamic Stabilization of DC Microgrids," *IEEE Transactions on Industrial Electronics*, vol. 66, DOI: 10.1109/TIE.2018.2826485, no. 2, 2019.
- [28] S. Yousefzadeh, N. Vafamand, J. D. Bendtsen, M. H. Khooban, F. Blaabjerg, and T. Dragičević, "Online Power Estimation of non-ideal CPLs in Shipboard DC MGs Using Cubature Kalman Filter," accepted in the 2nd European Conference on Electrical Engineering & Computer Science, Bern, Switzerland, 2018.
- [29] H. Jianjun, Z. Jiali, and J. Feng, "A CKF based spatial



alignment of radar and infrared sensors,” in *10<sup>th</sup> IEEE International Conference on Signal Processing (ICSP)*, DOI: 10.1109/ICOSP.2010.5655101, pp. 2386–2390, 2010.

- [30] G. Welch and G. Bishop, “An Introduction to the Kalman Filter,” in *Proc of SIGGRAPH, Course*, 8, no. 27599-3175, p. 81, Aug. 2001.



**Shirin Yousefizadeh** was born in Iran in 1990. She received her B.Sc. and M.Sc. degrees in control engineering in 2012 and 2015 from Iran University of Science and Technology, Iran, and Shiraz University of Technology, Iran, respectively. Since 2016, she has been a Ph.D. student in the Department of Electronic Systems, Aalborg University, Denmark.

Her main research interests include nonlinear control theory and applications, fault tolerant control systems, collaborative robotics, and stability and control of power systems. She is an active reviewer of several IEEE journals.



**Jan Dimon Bendtsen** (M'11) was born in Denmark in 1972. He received the M.Sc. degree in adaptive control using artificial neural networks and the Ph.D. degree in neural modeling and control of thermodynamic processes in thermal power plants from the Department of Control Engineering, Aalborg University, Aalborg, Denmark, in 1996 and 1999, respectively.

Since 2003, he has been an Associate Professor with the Department of Electronic Systems, Aalborg University. In 2005, he was a Visiting Researcher with Australian National University, Canberra, ACT, Australia. Since 2006, he has been involved in the management of several national and international research projects, and organizing international conferences. From 2012 to 2013, he was a Visiting Researcher with the University of California at San Diego, USA.

His current research interests include adaptive control of nonlinear systems, closed-loop system identification, control of distribution systems, and infinite-dimensional systems.

Dr. Bendtsen was a corecipient of the Best Technical Paper Award at the American Institute of Aeronautics and Astronautics Guidance, Navigation, and Control Conference in 2009.



**Navid Vafamand** received his B.Sc. degree in electrical engineering and M.Sc. degree in control engineering from Shiraz University of Technology, Iran, in 2012 and 2014, respectively. He is a Ph.D. candidate in control engineering in Shiraz University, Iran. Currently, he is a Ph.D. visiting student at Aalborg University, Denmark.

His main research interests include Takagi-Sugeno (TS) fuzzy models, linear parameter varying (LPV) systems, predictive control, and stability and control DC microgrids.

Dr. Vafamand has published more than 50 publications on journals and conferences, plus one book chapter.



**Mohammad-Hassan Khooban** (M'13-SM'18) was born in Shiraz, Iran, in 1988. He received the Ph.D. degree from Shiraz University of Technology, Shiraz, Iran, in 2017. He was a research assistant with the University of Aalborg, Aalborg, Denmark from 2016 to 2017 conducting research on Microgrids and Marine Power

Systems. Currently, he is a PostDoctoral Associate at Aalborg University, Denmark.

His research interests include control theory and application, power electronics and its applications in power systems, industrial electronics, and renewable energy systems.

Dr. Khooban is author or co-author of more than 100 publications on journals and international conferences, plus one book chapter and one patent. He is currently serving as an Associate Editor of the Complexity Journal.



**Frede Blaabjerg** (S'86–M'88–SM'97–F'03) was with ABB-Scandia, Randers, Denmark, from 1987 to 1988. From 1988 to 1992, he got the PhD degree in Electrical Engineering at Aalborg University in 1995. He became an Assistant Professor in 1992, an Associate Professor in 1996, and a Full Professor of power electronics and drives in 1998. From 2017 he became a Villum Investigator. He is honoris causa at University Politehnica Timisoara (UPT), Romania and Tallinn Technical University (TTU) in Estonia.

His current research interests include power electronics and its applications such as in wind turbines, PV systems, reliability, harmonics and adjustable speed drives. He has published more than 600 journal papers in the fields of power electronics and its applications. He is the co-author of four monographs and editor of ten books in power electronics and its applications.

Prof. Blaabjerg has received 28 IEEE Prize Paper Awards, the IEEE PELS Distinguished Service Award in 2009, the EPE-PEMC Council Award in 2010, the IEEE William E. Newell Power Electronics Award 2014 and the Villum Kann Rasmussen Research Award 2014. He was the Editor-in-Chief of the IEEE TRANSACTIONS ON POWER ELECTRONICS from 2006 to 2012. He has been Distinguished Lecturer for the IEEE Power Electronics Society from 2005 to 2007 and for the IEEE Industry Applications Society from 2010 to 2011 as well as 2017 to 2018. In 2018 he is President Elect of IEEE Power Electronics Society. He serves as Vice-President of the Danish Academy of Technical Sciences. He is nominated in 2014, 2015, 2016 and 2017 by Thomson Reuters to be between the most 250 cited researchers in Engineering in the world.



**Tomislav Dragičević** (S'09-M'13-SM'17) received the M.Sc. and the industrial Ph.D. degrees in Electrical Engineering from the Faculty of Electrical Engineering, Zagreb, Croatia, in 2009 and 2013, respectively. From 2013 until 2016 he has been a Postdoctoral research associate at Aalborg University, Denmark. From March 2016 he is an Associate Professor at Aalborg University, Denmark. He made a guest professor stay at Nottingham University, UK during spring/summer of 2018.

His principal field of interest is overall system design of autonomous and grid connected DC and AC microgrids, and application of advanced modeling and control concepts to power electronic systems.

Dr. Tomislav has authored and co-authored more than 140 technical papers (more than 55 of them are published in international journals, mostly IEEE Transactions) in his domain of interest and 8 book chapters and a book in the field. He serves as an Associate Editor in the IEEE TRANSACTIONS ON INDUSTRIAL ELECTRONICS and in the Journal of Power Electronics. Dr. Dragičević is a recipient of a Končar prize for the best industrial PhD thesis in Croatia, and a Robert Mayer Energy Conservation award.